

# Photoreactivity of Self-assembled Monolayers of Azobenzene or Stilbene Derivatives Capped on Colloidal Gold Clusters

Jian Zhang, James K. Whitesell,\* and Marye Anne Fox\*

Department of Chemistry, North Carolina State University, Raleigh, North Carolina 27695

Received September 19, 2000. Revised Manuscript Received December 19, 2000

*Trans*-4-methyl-4'-(–S–(CH<sub>2</sub>)<sub>n</sub>–O–)azobenzenes (**1**) with varying alkyl chain lengths ( $n = 4, 6, 9, 12$ ) and *trans*-4-methyl-4'-(–S–(CH<sub>2</sub>)<sub>n</sub>–O–)stilbenes (**2**) ( $n = 6, 7, 8, 9$ ) were used to cap colloidal gold clusters, yielding composite shell–core nanostructures **3** and **4**, respectively. Aggregation of the terminal arene moieties by  $\pi$ -stacking within the organic shells was weak in these composite particles. Upon irradiation at 350 nm, photoisomerization of the appended *trans* isomer to the corresponding *cis* isomer takes place both in solution and in the composite cluster. Inefficient photodimerization could be observed by <sup>1</sup>H NMR spectroscopy for cluster **4**. The quantum yields for photoisomerization of the composite clusters **3** and **4** were affected by the length of the linker because of distance-dependent through-bond quenching by the metal core.

## Introduction

The synthesis and characterization of electro- and photoactive self-assembled monolayers (SAM) of functionalized thiols on noble metal surfaces is important in developing next-generation optical and electronic materials.<sup>1–5</sup> It is of special interest to examine differences in excited-state behavior observed when a photoresponsive shell molecule is bound to the periphery of a colloidal metal nanoparticle instead of to a flat noble metal surface.<sup>2,3,6,7</sup> Surface irregularities in the resulting shell–core nanoparticle may influence photo-

responsiveness because of variance in local packing or lower local density of bound probe molecules. A thiolate-capped colloidal gold particle can be viewed as a metallic core comprised of edges and locally flat metal facets of different sizes to which the organic thiolate is bound, producing a loosely packed array of self-assembled organic side chains (Figure 1).<sup>3a</sup>

Composite shell–core clusters can often be dispersed as an apparently homogeneous suspension. Extensive spectroscopic characterization of such surface-capped gold clusters has shown that the micromorphology of these arrays often mimics that observed for a SAM on flat polycrystalline gold,<sup>2</sup> although the curvature of the smaller facets permits greater local conformational flexibility. The effect of the metallic cluster on the photochemistry of chromophores present in the capping group can then be investigated as a means for controlling those materials properties that depend on local order.<sup>8–10</sup>

The length and chemical composition of the linker separating the terminal chromophore from the Au support may also affect the photochemical reactivity of the photoactive group present in the appended SAM. First, varying the chain length of the spacer in a thiol-capped Au cluster may induce conformational changes that affect local order<sup>11,12</sup> because of cumulative differences in interchain packing forces. Second, variation in chain length can influence the magnitude of through-bond coupling between the chromophore and the metal core. Although excited states can be quenched near a

(1) (a) Abbott, N. L.; Folkers, J. P.; Whitesides, G. M. *Science* **1992**, *257*, 1380. (b) Lopez, G. P.; Biebuyck, H. A.; Frisbie, C. D.; Whitesides, G. M. *Science* **1993**, *258*, 647. (c) Wollman, E. W.; Kang, D.; Frisbie, C. D.; Lorkovic, I. M.; Wrighton, M. S. *J. Am. Chem. Soc.* **1994**, *116*, 4395. (d) Wolf, M. O.; Fox, M. A. *J. Am. Chem. Soc.* **1995**, *117*, 1845. (e) Fox, M. A.; Wooten, M. D. *Langmuir* **1997**, *13*, 7099.

(2) (a) Templeton, A. C.; Hostetler, M. J.; Kraft, C. T.; Murray, R. W. *J. Am. Chem. Soc.* **1998**, *120*, 1906. (b) Templeton, A. C.; Hostetler, M. J.; Warmoth, E. K.; Chen, S.; Hartshorn, C. M.; Krishnamurthy, V. M.; Forbes, M. D. E.; Murray, R. W. *J. Am. Chem. Soc.* **1998**, *120*, 4845. (c) Templeton, A. C.; Wuelfing, W. P.; Murray, R. W. *Acc. Chem. Res.* **2000**, *33*, 27.

(3) (a) Whetten, R. L.; Khoury, J. T.; Alvarez, M. M.; Murthy, S.; Vezmar, I.; Wang, Z. L.; Stephens, P. W.; Cleveland, C. L.; Luedtke, W. D.; Landman, U. *Adv. Mater.* **1996**, *8*, 428. (b) Arnold, R. J.; Reilly, J. P. *J. Am. Chem. Soc.* **1998**, *120*, 1528. (c) Badia, A.; Cuccia, L.; Demers, L.; Morin, F.; Lennox, R. B. *J. Am. Chem. Soc.* **1997**, *119*, 2682. (d) Brust, M.; Walker, M.; Bethell, D.; Schiffrin, D. J.; Whyman, R. *J. Chem. Soc., Chem. Commun.* **1994**, 801.

(4) Li, W.; Lynch, V.; Thompson, H.; Fox, M. A. *J. Am. Chem. Soc.* **1997**, *119*, 7211.

(5) (a) Wolf, M. O.; Fox, M. A. *Langmuir* **1996**, *12*, 955. (b) Reese, S.; Fox, M. A. *J. Phys. Chem. B* **1998**, *102*, 9820. (c) Fox, M. A.; Whitesell, J. K.; McKerrow, A. *J. Langmuir* **1998**, *14*, 816.

(6) (a) Allara, D. *Characterization of Organic Thin Films*; Ulman, A., Ed.; Butterworth-Heinemann: Boston, 1995; Chapter 4. (b) Ulman, A. *Ulthathin Organic Films*; Academic Press: San Diego, 1991. (c) Ulman, A. *Chem. Rev.* **1996**, *96*, 1533.

(7) (a) Brown, L. O.; Hutchison, J. E. *J. Am. Chem. Soc.* **1997**, *119*, 1238. (b) Fink, J.; Kiely, C. J.; Bethell, D.; Schiffrin, D. J. *Chem. Mater.* **1998**, *10*, 922. (c) Brust, M.; Walker, M.; Bethell, D.; Schiffrin, D. J.; Whyman, R. *J. Chem. Soc., Chem. Commun.* **1994**, 801. (d) Buining, P. A.; Humbel, B. M.; Philpse, A. P.; Verkleij, A. J. *Langmuir* **1997**, *13*, 3921. (e) Schmid, G. *Inorg. Synth.* **1990**, *27*, 214.

(8) (a) Badia, A.; Singh, S.; Demers, L.; Brown, G. R.; Lennox, R. B. *Chem. Eur. J.* **1996**, *2*, 359. (b) Badia, A.; Back, R.; Lennox, R. B. *Angew. Chem., Int. Ed. Engl.* **1994**, *3*, 2332.

(9) (a) Hostetler, M. J.; Stokes, J. J.; Murray, R. W. *Langmuir* **1996**, *12*, 3604. (b) Aguilera, A.; Murray, R. W. *Langmuir* **2000**, *16*, 5949.

(10) Schmitt, J.; Mächtle, P.; Eck, D.; Möhwald, H.; Helm, C. A. *Langmuir* **1999**, *15*, 3256.

(11) Badia, A.; Lennox, R. B.; Reven, L. *Acc. Chem. Res.* **2000**, *33*, 475.

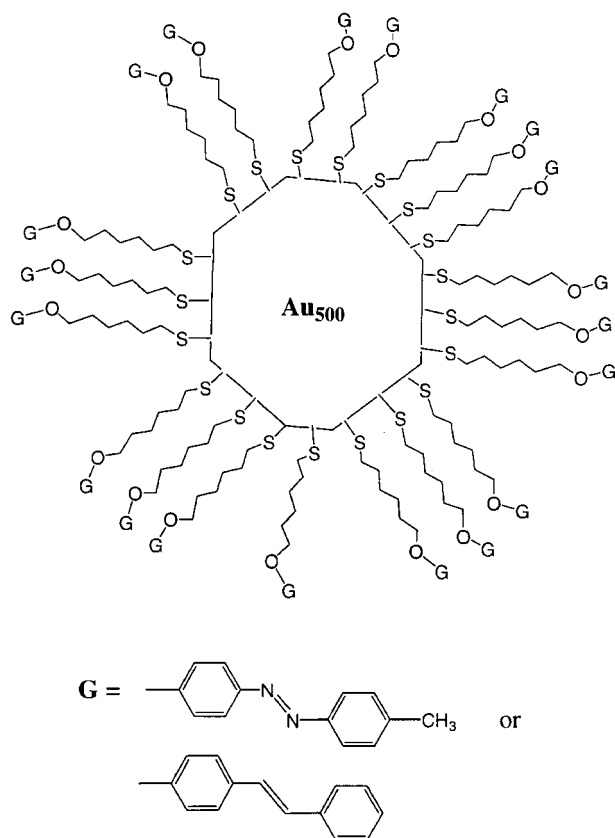


**Figure 1.** Schematic representation of a thiol-capped gold cluster emphasizing the variation in metal facet size.

metal surface through direct electron transfer or through dipolar coupling via an image electron-hole pair,<sup>13</sup> this quenching is incomplete,<sup>4,5</sup> for net emission and/or photochemical reactivity can be observed. Electron transfer from a donor to an acceptor generally takes place through electronic coupling through the molecular framework,<sup>14</sup> so the linker length may be a key factor in controlling the quantum yields of emission or chemical reaction.<sup>15</sup>

In this paper, we compare the photoefficiency of geometric isomerization in two families of shell-core nanoclusters **3** and **4** capped with organic thiols end-bound with an azobenzene **1** or a stilbene **2** chromophore.<sup>16</sup> In these clusters, the photoactive group is separated by a thiol-terminated alkyl chain of variable length from a gold cluster of a fixed size (Au<sub>500</sub>). Azobenzene and stilbene derivatives are exquisitely sensitive to the topology of molecular aggregation, both in the solution and in the solid state.<sup>17-22</sup> In solution, reversible photoisomerization of the precursor trans isomer **1** or **2** to the corresponding cis isomer takes place

upon direct excitation,<sup>23-27</sup> and analogous transformations are also observed for the bound chromophores in clusters **3** and **4**, respectively. Photodimerization of the appended stilbenes is also expected when these groups are tightly packed in crystals, microemulsions, or Langmuir-Blodgett films.<sup>5a,18,28</sup>

We report here the dependence on spacer length of the observed quantum yields for trans to cis isomerization in clusters **3** and **4**. We explain why the trans-to-cis photoisomerization of an analogous stilbene as a monolayer on planar gold is blocked because of high crystallinity and dense packing of the monolayer,<sup>5a</sup> whereas trans-to-cis photoisomerization in clusters **3** and **4** can take place readily.<sup>16</sup> Monitoring excited-state partitioning between these two processes will provide valuable information about optoelectronic characteristics of these novel photoresponsive shell-core clusters.

## Experimental Section

**1. Materials and General Techniques.** Chemical reagents (Aldrich) were used as received. All solvents were

(17) (a) Görner, H.; Kunh, H. J. *Adv. Photochem.* **1995**, *19*, 1. (b) Turro, N. J. *Modern Molecular Photochemistry*; Benjamin-Cummings Publishing Co.: New York, 1978. (c) Murov, S. L.; Carmichael, I.; Hug, G. L. *Handbook of Photochemistry*, 2nd ed.; Marcel Dekker: New York, 1993.

(18) Whitten, D. G.; Chen, L.; Geiger, H. C.; Perlstein, J.; Song X. *J. Phys. Chem. B* **1998**, *102*, 10098.

(19) (a) Song X.; Perlstein, J.; Whitten, D. G. *J. Phys. Chem. A* **1998**, *102*, 5440. (b) Song X.; Perlstein, J.; Farahat, M.; Perlstein, J.; Whitten, D. G. *J. Am. Chem. Soc.* **1997**, *119*, 9144.

(20) Rau, H.; Liddecke, E. *J. Am. Chem. Soc.* **1982**, *104*, 1616. (b) Rau, H. In *Photochromism: Molecules and Systems*; Dürr, H., Bouas-Laurent, H., Eds; Elsevier: Amsterdam, 1990.

(21) (a) Ishihara, K.; Namada, N.; Kato, S.; Shinohara, I. *J. Polym. Sci., Polym. Chem. Ed.* **1984**, *22*, 121. (b) Ishihara, K.; Namada, N.; Kato, S.; Shinohara, I. *J. Polym. Sci., Polym. Chem. Ed.* **1983**, *21*, 1551.

(22) Okahata, Y.; Fujita, S.; Iizuka, N. *Angew. Chem., Int. Ed. Engl.* **1986**, *25*, 751.

(23) (a) Liu, Z. F.; Hashimoto, K.; Fujishima, A. *Nature* **1990**, *347*, 18. (b) Gibbons, W. M.; Shannon, P. J.; Sun, S.-T.; Swetlin, B. J. *Nature* **1991**, *351*, 49. (c) Campbell D. J.; Herr, B. R.; Hulteen, J. C.; Van Duyne, R. P.; Mirkin, C. A. *J. Am. Chem. Soc.* **1996**, *118*, 10211. (d) Wang, R.; Iyoda, T.; Tryk, D. A.; Hashimoto, K.; Fujishima, A. *Langmuir* **1997**, *13*, 4644.

(24) (a) Geiger, H. C.; Pertein, J.; Lachicotte, R. J.; Wyrozebski, K.; Whitten, D. G. *Langmuir* **1999**, *15*, 5606. (b) Hong, J.-D.; Park, E.-S.; Park, A.-L. *Langmuir* **1999**, *15*, 6515. (c) Wu, Y.; Mamiya, J.; Kanazawa, A.; Shiono, T.; Ikeda, T.; Zhang, Q. *Macromolecules* **1999**, *32*, 8829. (d) Meier, J. G.; Ruhmann, R.; Stumpe, J. *Macromolecules* **2000**, *33*, 843. (e) Engelking, J.; Wittmann, M.; Rehahn, M.; Menzel, H. *Langmuir* **2000**, *16*, 3407. (f) Tsuda, K.; Dol, G. C.; Gensch, T.; Hofkens, J.; Latterini, L.; Weener, J. W.; Meijer, E. W.; De Schryver, F. C. *J. Am. Chem. Soc.* **2000**, *122*, 3445.

(25) (a) Ikeda, T.; Tsutsumi, O. *Science* **1995**, *268*, 1873. (b) Brown, C. L.; Jonas, U.; Preece, J. A.; Ringsdorf, H.; Seitz, M.; Stoddart, J. F. *Langmuir* **2000**, *16*, 1924. (c) Astrand, P.-O.; Ramanujam, P. S.; Hvilsted, S.; Bak, K. L.; Sauer, S. P. A. *J. Am. Chem. Soc.* **2000**, *122*, 3482.

(26) (a) Willner, I.; Rubin, S.; Riklin, A. *J. Am. Chem. Soc.* **1991**, *113*, 3321. (b) Lednev, I. K.; Ye, T.-Q.; Abbott, L. C.; Hester, R. E.; Moore, J. N. *J. Phys. Chem. A* **1998**, *102*, 9161. (c) Seki, T.; Fukuchi, T.; Ichimura, K. *Langmuir* **2000**, *16*, 3564.

(27) (a) Caldwell, W. B.; Campbell, D. J.; Chen, K.; Herr, B. R.; Mirkin, C. A.; Malik, A.; Durbin, M. K.; Dutta, P.; Huang, K. G. *J. Am. Chem. Soc.* **1995**, *117*, 6071. (b) Campbell, D. J.; Herr, B. R.; Hulteen, J. C.; Van Duyne, R. P.; Mirkin, C. A. *J. Am. Chem. Soc.* **1996**, *118*, 10211. (c) Ye, Q.; Fang, J.; Sun, L. *J. Phys. Chem. B* **1997**, *101*, 8221. (d) Yu, H.-Z.; Wang, Y.-Q.; Cheng, J.-Z.; Zhao, J.-W.; Cai, S.-M.; Inokuchi, H.; Fujishima, A.; Liu, Z.-F. *Langmuir* **1996**, *12*, 2843. (e) Tamada, K.; Nagasawa, J.; Nakanishi, F.; Abe, K. *Langmuir* **1998**, *14*, 3264. (f) Han, S. W.; Kim, C. H.; Hong, S. H.; Chung, Y. K.; Kim, K. *Langmuir* **1999**, *15*, 1579.

(28) (a) Schechter, H.; Link, W. J.; Tiers, G. V. D. *J. Am. Chem. Soc.* **1963**, *85*, 1601. (b) Coates, G. W.; Dunn, A. R.; Henling, L. M.; Ziller, J. W.; Lobkovsky, E. B.; Grubbs, R. H. *J. Am. Chem. Soc.* **1998**, *120*, 3641. (c) Mishra, B. K.; Valaulikar, B. S.; Kunjappu, T.; Manohar, C. *J. Colloid Interface Sci.* **1989**, *127*, 373. (d) Rao, K. S. S. P.; Hubig, S. M.; Moorthy, J. N.; Kochi, J. N. *J. Org. Chem.* **1999**, *64*, 8098. (e) Whitten, D. G. *Acc. Chem. Res.* **1993**, *26*, 502.

(12) (a) Porter, M. D.; Bright, T. B.; Allara, D. L.; Chidsey, C. E. D. *J. Am. Chem. Soc.* **1987**, *109*, 3559. (b) Nuzzo, R. G.; Dubois, L. H.; Allara, D. L. *J. Am. Chem. Soc.* **1990**, *112*, 558. (c) Camillone, N.; Chidsey, C. E. D.; Liu, G. Y.; Putviniski, T. M.; Scoles, G. *J. Chem. Phys.* **1991**, *94*, 8493. (d) Chidsey, C. E. D.; Liu, G. Y.; Rowntree, P.; Scoles, G. *J. Chem. Phys.* **1989**, *91*, 4421.

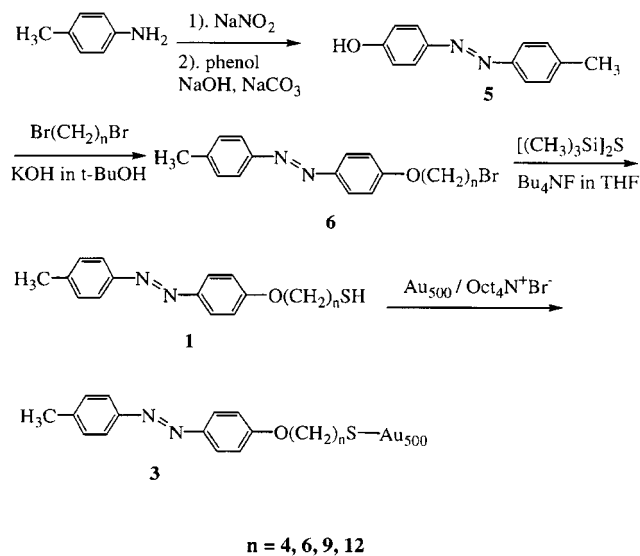
(13) Nordlander, P. In *Laser Spectroscopy and Photochemistry on Metal Surfaces, Part I*; Dai, H.-L., Ho, W., Eds.; World Science Press: Singapore, 1995; Chapter 9, p 347.

(14) Winkler, J. R.; Gray, H. B. *Chem. Rev.* **1992**, *92*, 369.

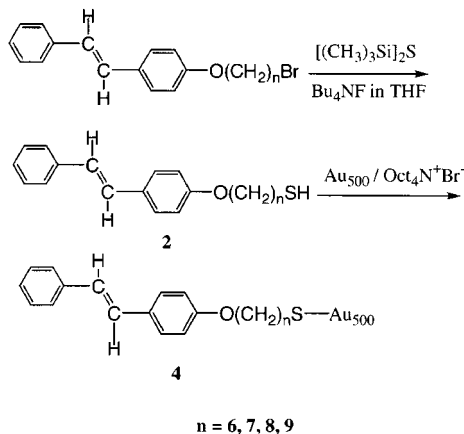
(15) Kittredge, K.; Whitesell, J. K.; Fox, M. A. *J. Phys. Chem.*, submitted.

(16) Hu, J.; Zhang, J.; Liu, F.; Kittredge, K.; Whitesell, J. K.; Fox, M. A. *J. Am. Chem. Soc.* **2001**, *123*, 1464.

### Scheme 1. Synthesis of Thiolate Azobenzene Derivatives 1 and Composites 3



### Scheme 2. Synthesis of Thiolate Stilbene Derivatives 2 and Composites 4



spectroscopic grade (Fisher or Aldrich). Water (Milli Q) used in the colloidal gold synthesis had a resistance of higher than 4 MW. Commercial solvents were used without further purification. Deuterated solvents were obtained from Isotech and Aldrich.

Air- and moisture-sensitive reactions were performed under an inert atmosphere ( $\text{N}_2$  or Ar that had been passed through a drierite tower). Glassware was oven-dried at 140 °C or flame-dried, if necessary. The progress of each reaction was monitored by thin-layer chromatography (TLC) carried out on 0.25-mm E. Merck silica gel plates (60F-254). Baxter silica gel (60 Å) (230–400 mesh ASTM) was used for flash column chromatography.

**2. Synthesis of Thiols 1 and 2.** *Trans*-4-methyl-4'-(mercaptoalkoxy)azobenzenes (**1**) were prepared according to the route shown in Scheme 1 and the corresponding hydrocarbon **2** was prepared through an analogous route shown in Scheme 2.<sup>29–31</sup> Synthetic details are available in the Supporting Information.

**3. Preparation of Clusters 3 and 4.** A colloidal gold suspension was prepared by reducing a dilute water/toluene solution of  $\text{HAuCl}_4$  with  $\text{NaBH}_4$  in the presence of tetraoctylammonium bromide.<sup>2</sup> Ligand exchange was induced by replac-

ing the tightly bound bromide ion with the desired thiol. Thiol **1** or **2** (10 mg) was added to 25 mL of a toluene solution of colloidal gold. The resulting solution was stirred under Ar at room temperature for 4 h to form a fully equilibrated thiolate monolayer. The solvent was removed under vacuum and the residue was washed with ethanol and acetone. A black solid collected on a 0.2-mm membrane filter was separated from the film by sonication in acetone. The purity of the capped cluster was monitored by  $^1\text{H}$  NMR and absorption spectra. After evaporation of the solvent, the thiol-coated cluster was redissolved in  $\text{CH}_2\text{Cl}_2$  or  $\text{CHCl}_3$ .

**4. Photoreactivity.** Photochemical reactions were carried out with phosphor-coated low-pressure mercury arcs blazed at 350 nm in a Rayonet Photochemical Reactor (Southern New England Ultraviolet). Thiols **1** or **2** or capped clusters **3** or **4** were dissolved in  $\text{CH}_2\text{Cl}_2$  to produce  $10^{-5}$  M solutions, which were deaerated by bubbling with Ar for 15 min. The photo-reactions were monitored by absorption spectroscopy, fluorescence spectroscopy, and  $^1\text{H}$  NMR. The quantum yield ( $\Phi$ ) for isomerization or dimerization was determined against a benzophenone-benzhydrol actinometer.<sup>32</sup> By extrapolation of the plot of the measured  $\Phi$  at various times to time zero, an intrinsic quantum yield was determined.

## Results and Discussion

**1. Formation and Spectral Characterization of Thiol-Capped Gold Clusters.** A standard route to thiol-capped gold clusters involves treatment of a dilute  $\text{HAuCl}_4$  solution with sodium borohydride or sodium citrate in the presence of the capping thiol.<sup>33</sup> Because thiols **1** and **2** are susceptible to reductive decomposition, however, ligand exchange of a thiol for the bromide ion tightly bound to the metallic cluster was employed.<sup>34</sup> Our colloid preparation followed the procedure of Brust and co-workers, with replacement of tetraoctylammonium bromide by thiol taking place after Au core formation.<sup>3d</sup> Transmission electron microscopy showed cluster distributions identical to those reported in this earlier work. Therefore, the diameters of the colloidal gold clusters prepared by this method range from 1.5 to 3.5 nm, centered at about 2.5 nm, containing about 500 Au atoms in a cluster capped by about 100 thiol molecules.<sup>3a,b</sup>

The surface of a colloidal Au cluster consists of Au(111) subflats of a range of sizes.<sup>2</sup> Because a cluster containing 500 gold atoms has roughly the dimensions of a cube with 8 atoms on an edge, the facet sizes for an  $\text{Au}_{500}$  core are necessarily fairly small. High densities of surface irregularities or step edges and an abundance of small metal facets of the gold nanoparticle dictate that some thiols are bound near facet edges. The thiols on small subflats would aggregate more weakly than those bound on a larger flat facet because long-range packing forces will be weak. According to the results of  $^1\text{H}$  NMR and FTIR spectroscopy, no residual tetraoctylammonium bromide (<5%, from the detection limits

(32) Moore, W. M.; Ketchum, M. *J. Am. Chem. Soc.* **1962**, *84*, 1368.

(33) (a) Turkevich, J.; Stevenson, P. C.; Hillier, J. *Discuss. Faraday Soc.* **1951**, *11*, 55. (b) Faraday, M. *Philos. Trans. R. Soc. London* **1957**, *147*, 145. (c) Cunnane, V. J.; Schiffrin, D. J.; Beltran, C.; Gebeltran, G.; Solomon, T. *J. Electroanal. Chem.* **1988**, *247*, 145. (d) Thomas, J. M. *Pure Appl. Chem.* **1988**, *60*, 1517. (e) Edwards, P. P. *Mater. Res. Soc. Symp. Proc.* **1992**, *272*, 311. (f) Hosteler, M. J.; Wingate, J. E.; Zhong, C.-J.; Harris, J. E.; Vachet, R. W.; Clark, M. R.; London, J. D.; Green, S. J.; Stokes, J. J.; Wignall, G. D.; Glish, G. L.; Proter, M. D.; Evans, N. D.; Murray, R. W. *Langmuir* **1998**, *14*, 17.

(34) (a) Porter, M. D.; Bright, T. B.; Allara, D. L.; Chidsey, C. E. D. *J. Am. Chem. Soc.* **1987**, *109*, 3559. (b) Linbinis, P. E.; Muzzo, R. G.; Whitesides, G. M. *J. Phys. Chem.* **1992**, *96*, 5097.

(29) Sandhu, S. S.; Yianni, Y. P.; Morgan, C. G.; Taylor, D. M.; Zaba, B. *Biochim. Biophys. Acta* **1986**, *860*, 253.

(30) Hu, J.; Fox, M. A. *J. Org. Chem.* **1999**, *64*, 4959.

(31) Wyrzykiewicz, E.; Wybieralska, J.; Grzesiak, J.; Prukala, W. *Pol. J. Chem.* **1990**, *64*, 323.



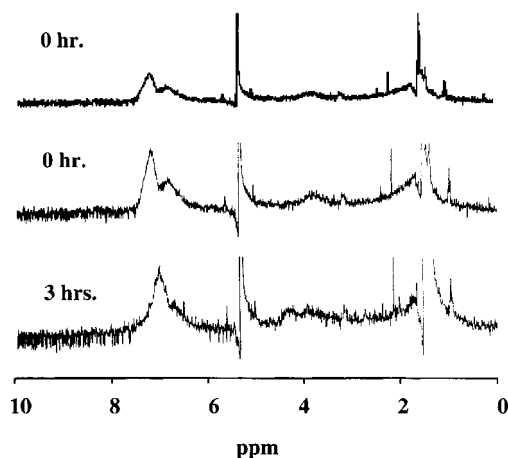


**Figure 2.**  $^1\text{H}$  NMR spectra of cluster **4** ( $n = 9$ ) in degassed  $\text{CD}_2\text{Cl}_2$  before (top, complete spectrum; middle, expanded spectrum) and after (bottom) 3 h of irradiation at 350 nm.

of these techniques) remains on the Au core after replacement by thiol. Instead, differences in surface packing density on these shell–core composites and in a self-assembled monolayer on an evaporated gold surface were likely caused by incomplete surface coverage, as has been demonstrated for chromophores packed more loosely on a Au cluster than on a flat Au surface.<sup>2</sup> If so, average  $\pi$ -stacking of chromophores on the colloidal Au core will be weaker. Incomplete surface coverage by thiols or the presence of surface defects would also contribute to loose packing on the surface of this shell–core nanocomposite.

Figure 2 shows a  $^1\text{H}$  NMR spectrum of cluster **4**,  $n = 9$ . The peaks typical of the precursor **2**,  $n = 9$ , were broadened and overlapped in the cluster, indicating that the thiol molecules were packed on the surface of the  $\text{Au}_{500}$  core and that their motions were restricted.<sup>9,35</sup> The peak broadening caused by the restricted motion of the bound stilbene moieties produced significant spectral overlap. Analogous spectral features were observed for clusters **3**,  $n = 4, 6, 9, 12$ , and for clusters **4**,  $n = 6, 7, 8$ .

The transmission FT-IR spectrum of cluster **3** ( $n = 9$ ) shows peaks characteristic of thiol **1** ( $n = 9$ ) (Figure 3). Because the transmission of the C–O stretching peaks ( $1225$  and  $1270\text{ cm}^{-1}$ ) became attenuated upon binding to the colloidal Au core, the thiol molecules were believed to have packed tightly at about a  $30^\circ$  angle from the surface of the Au core.<sup>35,36</sup> Clusters **3**,  $n = 4, 6, 12$ , and clusters **4**,  $n = 6, 7, 8, 9$ , showed similar characteristic transmission FT-IR stretches to those observed with cluster **3**,  $n = 9$ .

Thiols **1** and **2** displayed a remarkable decrease in solubility in organic solvents upon increasing the linker length  $n$ . The thiolate-capped gold clusters **3** and **4** also showed the same tendency. Solubility was thus regulated mainly by the capping reagent.

(35) (a) Brousseau, L. C.; Zhao, Q.; Shultz, D. A.; Feldheim, D. L. *J. Am. Chem. Soc.* **1998**, *120*, 7645. (b) Grabar, K. C.; Freeman, R. G.; Hommer, M. B.; Natan, M. J. *Anal. Chem.* **1995**, *67*, 735. (c) Hayat, M. A., Ed. *Colloidal Gold: Principles, Methods, and Applications*; Academic Press: San Diego, CA, 1991.

(36) (a) Dubois, L. H.; Nuzzo, R. G.; *Annu. Rev. Phys. Chem.* **1992**, *43*, 437. (b) Bain, C. D.; Whitesides, G. M. *Angew. Chem., Int. Ed. Engl.* **1989**, *28*, 506. (c) Nordlander, P. In *Laser Spectroscopy and Photochemistry on Metal Surfaces, Part I*; Dai, H.-L., Ho, W., Eds.; World Science Press: Singapore, 1995; Chapter 9, p 347.

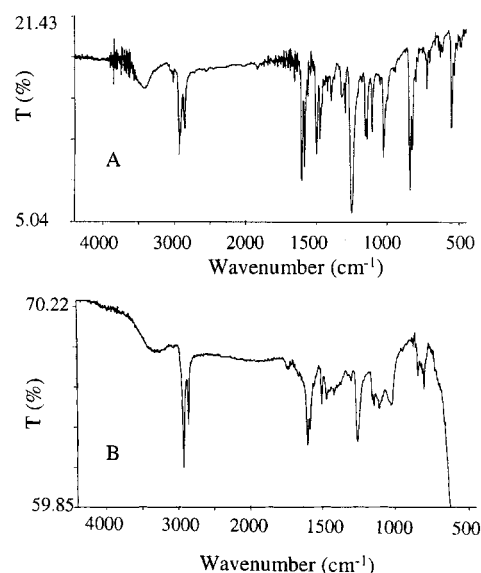


**Figure 3.** Transmission FT-IR spectroscopy of (A) azobenzene **1** ( $n = 9$ ) and (B) a cluster **3** ( $n = 9$ ) as KBr pellets.

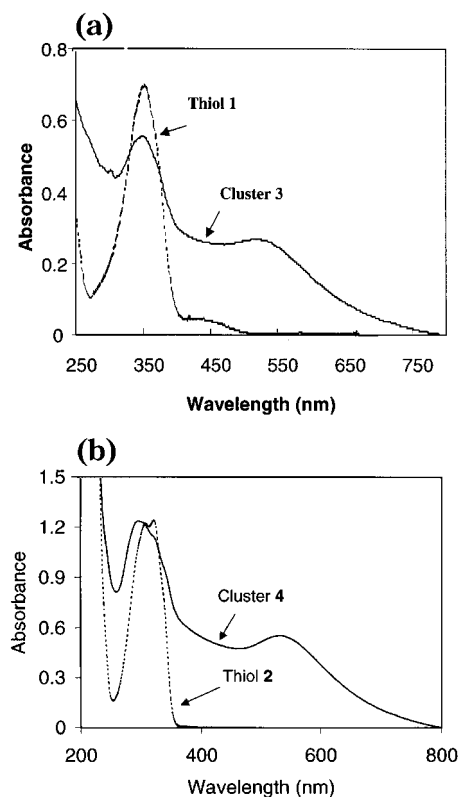


**Figure 4.** Absorption spectra of (a) azobenzene **1** ( $n = 9$ ,  $2.5 \times 10^{-5}\text{ M}$ ) and cluster **3** ( $n = 9$ ,  $2.0 \times 10^{-5}\text{ M}$ ) and (b) stilbene **2** ( $n = 9$ ,  $3.3 \times 10^{-5}\text{ M}$ ) and cluster **4** ( $n = 9$ ,  $3.0 \times 10^{-5}\text{ M}$ ) in degassed  $\text{CH}_2\text{Cl}_2$ .

*Trans*-azobenzene **1**,  $n = 9$ , exhibits a weak  $n,\pi^*$  transition at 430 nm and an intense  $\pi,\pi^*$  transition at 351 nm (Figure 4a). Stilbene **2**,  $n = 9$ , exhibited an intensive  $\pi,\pi^*$  transition at 307 nm (Figure 4b). These features are similar to those of their parent compounds.<sup>18,19</sup>

The Au colloid stabilized by tetraoctylammonium bromide displayed a broadened plasmon band with a maximum near 530 nm.<sup>2,8</sup> The plasmon bands in **3** and **4** were slightly blue-shifted, consistent with covalent bonding of a reagent to the cluster surface. Cluster **3**,  $n$

**Table 1. Quantum Yields of Isomerization and Dimerization of Azobenzene Derivatives 1 or Clusters 3 and Stilbene Derivatives 2 and Clusters 4 in Degassed CH<sub>2</sub>Cl<sub>2</sub> Solution (10<sup>-5</sup> M) upon Photolysis at 350 nm**

system	absorption $\lambda_{\max}$ (nm)	emission $\lambda_{\max}$ (nm)	isomerization ( $\Phi_i$ )	relative yield <sup>a</sup> ( $\Phi_i$ ) <sub>1 or 2</sub> / <sub>(<math>\Phi_i</math>)<sub>3 or 4</sub></sub>	dimerization ( $\Phi_d \times 10^6$ )
<b>1</b> , $n = 4$	351		$(1.0 \pm 0.1) \times 10^{-1}$		0
$n = 6$	350		$(1.0 \pm 0.1) \times 10^{-1}$		0
$n = 9$	351		$(1.1 \pm 0.1) \times 10^{-1}$		0
$n = 12$	351		$(1.0 \pm 0.1) \times 10^{-1}$		0
<b>3</b> , $n = 4$	345		$(7.3 \pm 2.3) \times 10^{-4}$	137	0
$n = 6$	344		$(6.5 \pm 2.0) \times 10^{-3}$	15	0
$n = 9$	346		$(3.7 \pm 0.6) \times 10^{-2}$	3.0	0
$n = 12$	345		$(6.7 \pm 2.2) \times 10^{-2}$	1.5	0
<b>2</b> , $n = 6$	307	373	$(3.3 \pm 0.8) \times 10^{-4}$		0
$n = 7$	306	373	$(3.4 \pm 0.7) \times 10^{-4}$		0
$n = 8$	306	373	$(3.3 \pm 0.8) \times 10^{-4}$		0
$n = 9$	307	374	$(3.4 \pm 0.8) \times 10^{-4}$		0
<b>4</b> , $n = 6$	301	378	$(5.7 \pm 1.4) \times 10^{-5}$	5.8	$2.2 \pm 0.8$
$n = 7$	299	379	$(1.3 \pm 0.4) \times 10^{-4}$	2.6	$3.4 \pm 0.9$
$n = 8$	301	378	$(1.6 \pm 0.4) \times 10^{-4}$	2.1	$3.8 \pm 1.1$
$n = 9$	300	378	$(2.1 \pm 0.7) \times 10^{-4}$	1.6	$4.3 \pm 1.2$

<sup>a</sup> Relative yield is defined as the ratio of the quantum yield of thiol 1 or 2 to that of cluster 3 or 4, respectively.

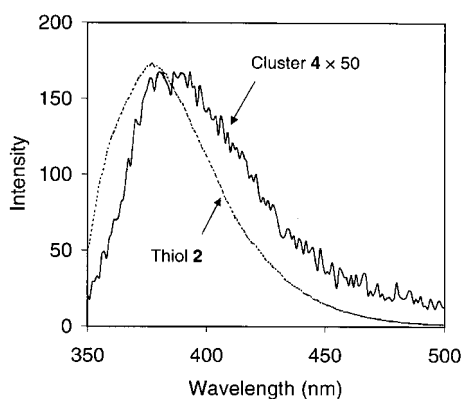


**Figure 5.** Fluorescence spectra of stilbene **2** ( $n = 9$ ,  $3.3 \times 10^{-5}$  M) and cluster **4** ( $n = 9$ ,  $3.0 \times 10^{-5}$  M) in degassed CH<sub>2</sub>Cl<sub>2</sub>.

$n = 9$ , exhibited  $\pi, \pi^*$  transition at 345 nm and cluster **4**,  $n = 9$ , at 300 nm (Figure 4a,b). The absorption maxima of azobenzene **1** and cluster **3** or stilbene **2** and cluster **4** were almost independent of linker length (Table 1). The absorption bands of clusters **3** and **4** were blue-shifted by 5–7 nm from those of **1** and **2**. Such shifts are consistent with surface attachment of the probe as a self-assembled monolayer and are incompatible with a fully intercalated structure.

When stilbene **2** was excited at 310 nm or cluster **4** at 300 nm, fluorescence was observed (373 nm for **2**,  $n = 9$ , and 378 nm for **4**,  $n = 9$  (Figure 5)). The fluorescence of cluster **4** was red-shifted by 4–6 nm from that of thiol **2** (Table 1). The fluorescence intensity of cluster **4** is enhanced upon increasing the linker length of the chain binding the stilbene chromophore to the Au core. No emission could be observed for either the azobenzene derivative **1** or cluster **3**.

Whitten and co-workers have observed a 25–30 nm blue-shift in the absorption maxima of both azobenzene and stilbene in bilayer assemblies from those seen with the freely solvated analogues in solution and a 30–40-nm red shift in the fluorescence maxima of the stilbenes.<sup>18,19</sup> They assign the blue shifts of the absorption maxima and the red shift of fluorescence maximum to aggregation caused by strong  $\pi$ - $\pi$  interactions. These reported shifts are much larger than those observed in capped clusters **3** and **4**. A significant dipolar interaction between the gold surface and the chromophore is

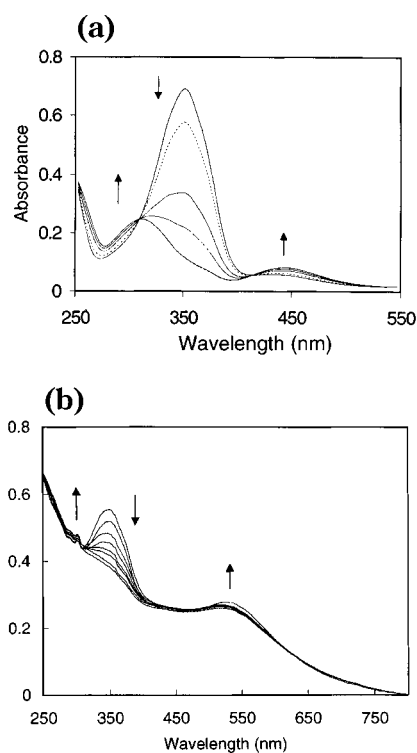


**Figure 6.** Changes in absorption spectra of (a) thiol **1** ( $n = 9$ ,  $2.5 \times 10^{-5}$  M) in degassed CH<sub>2</sub>Cl<sub>2</sub> upon photolysis at 350 nm for 12 s and (b) cluster **3** ( $n = 9$ ,  $2.0 \times 10^{-5}$  M) for 30 s.

probably responsible because a highly polar environment would stabilize the singlet excited state relative to the ground state, producing a red shift in the absorption maxima.<sup>37</sup> Weak  $\pi$ -stacking among adjacent moieties in the clusters **3** and **4** is also probable, as would be expected with loosely packed thiol arrays encasing the metallic core.

**2. Photoisomerization of Azobenzene in Thiols 1 and Clusters 3.** Photoisomerization from *trans*- to *cis*-azobenzene in thiol **1**,  $n = 9$ , in degassed CH<sub>2</sub>Cl<sub>2</sub> was monitored by absorption spectroscopy (Figure 6a) upon direct photolysis at 350 nm. Parallel reactions were also observed for **1**,  $n = 4, 6, 12$ . The  $\pi, \pi^*$  band at 351 nm decreased in intensity as the reaction proceeded, whereas

(37) Bortolus, P.; Monti, S. *J. Phys. Chem.* **1979**, *83*, 648.

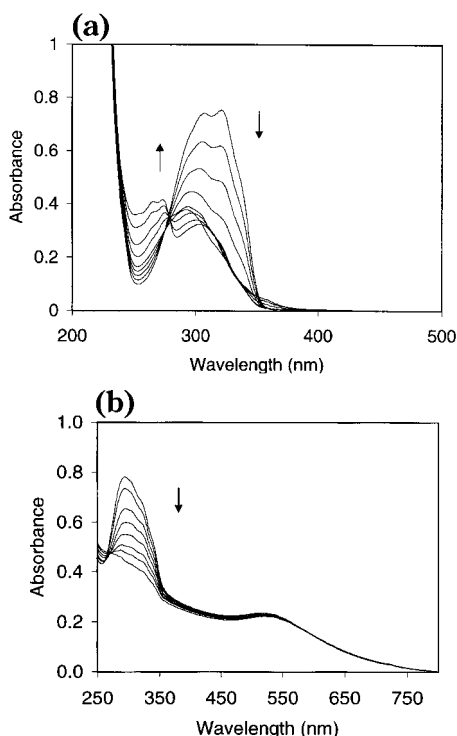


**Figure 7.** Changes in absorption spectra of (a) thiol **2** ( $n = 9$ ,  $2.1 \times 10^{-5}$  M) in degassed  $\text{CH}_2\text{Cl}_2$  upon photolysis at 350 nm for 40 min and (b) cluster **4** ( $n = 9$ ,  $2.0 \times 10^{-5}$  M) for 60 min.

the band at 306 nm rose simultaneously, producing an isobestic point at 308 nm. The  $n,\pi^*$  band was red-shifted from 430 to 442 nm and its intensity was enhanced. The final absorption spectrum closely resembles that of the parent *cis*-azobenzene,<sup>38</sup> indicating that *trans*-to-*cis* photoisomerization had occurred. We calculate from the observed spectral changes that almost all of the *trans* isomer was converted to the *cis* isomer in solution under these conditions. The quantum yields of photoisomerization  $(\Phi_i)_1$  for thiols **1** are independent of the length of the linker (Table 1).

Direct irradiation at 350 nm of cluster **3**,  $n = 9$ , displays a very similar reactivity to that observed for **1** in solution (Figure 6b). As with the soluble precursor, analogous reactivity was observed in clusters **3**,  $n = 4, 6, 12$ . The *trans*-azobenzene peak at 346 nm decreases with a simultaneous growth in intensity at about 300 nm, indicating a net production of the *cis* isomer. Changes in the isomeric composition were calculated from the absorption spectral changes. The quantum yields of isomerization for the clusters **3**  $(\Phi_i)_3$  increased markedly upon increasing the linker length, Table 1, but were still much lower than that for the corresponding thiols **1**.

**3. Competing Photoisomerization and Photodimerization of Stilbenes in Thiols **2** and Clusters **4**.** Photoisomerization of thiol **2**,  $n = 9$ , in  $\text{CH}_2\text{Cl}_2$  from the *trans* to the *cis* isomer was monitored with absorption (Figure 7a). The  $\pi,\pi^*$  bands at 307 nm decreased in intensity as the reaction proceeded, whereas the band at 269 nm rose simultaneously, producing an isobestic point at 278 nm. This observation was similar to the

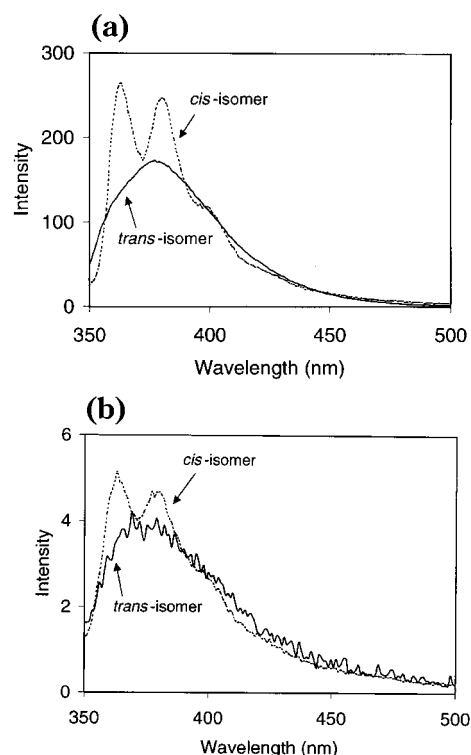


**Figure 8.** Changes in fluorescence spectra of (a) thiol **2** ( $n = 9$ ,  $2.1 \times 10^{-5}$  M) before (*trans*) and after (*cis*) photolysis at 350 nm in degassed  $\text{CH}_2\text{Cl}_2$  for 40 min and (b) cluster **4** ( $n = 9$ ,  $2.0 \times 10^{-5}$  M) for 60 min.

isomerization reported for the parent stilbene,<sup>5a,39</sup> implying that a *cis* isomer was formed.

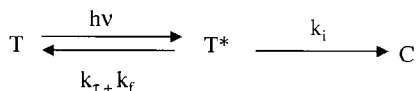
As before, analogous photoisomerization is observed for each of the other members of the series **2**, that is, for **2**,  $n = 6, 7, 8$ . This absorption spectral change provided evidence for the absence of a *trans* isomer in the final product mixture, indicating that almost all of the *trans* isomer had been converted to the *cis* isomer. The *cis* isomer exhibited two fluorescence bands at 362 and 379 nm (Figure 8a), whereas the *trans* isomer  $\pi,\pi^*$  band showed only a single broad emission. The quantum yield of geometric isomerization  $(\Phi_i)_2$  of thiol **2** was also independent of linker length (Table 1).

A mixture of possible [2 + 2] stilbene photodimerization products would be expected to exhibit tailing absorption near 250 nm and a chemical shift near 4.3 ppm in its  $^1\text{H}$  NMR spectrum.<sup>5a</sup> No such characteristics could be observed for the photoproducts derived from thiols **2** in solution, indicating that photodimerization did not occur in dilute solution. This is as expected because stilbene itself does not dimerize unless irradiated in highly concentrated solution or in the solid state.<sup>18,28</sup>

Cluster **4**,  $n = 9$ , was irradiated in degassed  $\text{CH}_2\text{Cl}_2$  at 350 nm under identical conditions. The plasmon absorption of the colloidal Au core overlapped the  $\pi,\pi^*$  band of the *cis* isomer. The absorption band at 300 nm assigned to the *trans* stilbene group decreased with a simultaneous growth in intensity at lower wavelengths

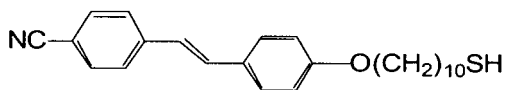
(38) (a) Zimmerman, G.; Chow, L.-Y.; Paik, U.-J. *J. Am. Chem. Soc.* **1958**, *80*, 3258. (b) Fischer, E. *J. Am. Chem. Soc.* **1960**, *82*, 3249.

(39) (a) Stermitz, F. R. In *Organic Photochemistry*, Chapman, O. L., Ed.; Marcel Dekker: New York, 1967; Vol. 1, p 247. (b) Saltiel, J.; D'Agostino, J.; Megarity, E. D.; Metts, L.; Neuberger, K. R.; Wrighton, M.; Zafiriou, O. C. In *Organic Photochemistry*, Chapman, O. L., Ed.; Marcel Dekker: New York, 1973; Vol. 3, p 1.

**Scheme 3. Photoreactions of 1 and 2 in Degassed CH<sub>2</sub>Cl<sub>2</sub> Solution upon Photolysis at 350 nm**


(Figure 7b). As with the analogous solution species, parallel reactivity was observed for **4**,  $n = 6, 7, 8$ . Changes in isomeric composition were calculated from the observed decrease of  $\pi, \pi^*$  absorption band of the trans isomer upon irradiation, assuming quantitative conversion to the cis isomer.

The fluorescence spectrum of the photoproduct derived from cluster **4**,  $n = 9$ , exhibited two bands at 379 and 362 nm (Figure 8b), as would be expected for the emission of the free cis isomer in solution. This observation supports the premise that geometric isomerization from *trans*- to *cis*-stilbene occurred on the cluster. It is also interesting that the *trans*-to-*cis* isomerization is observed in clusters **4** in solution, whereas the analogous *trans*-to-*cis* geometric photoisomerization is blocked in a self-assembled monolayer of thiol **7** capped on a flat

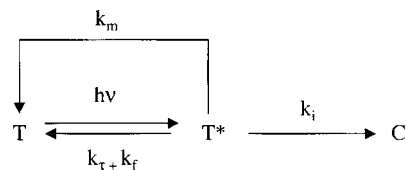

**7**

Au support.<sup>5a</sup> It is likely that tighter packing of the *trans*-stilbene groups of thiol **7** on a larger flat surface facet sterically blocks the isomerization. In contrast, the corresponding cluster **4** is less well-packed<sup>40</sup> and thiol **2** is bound to smaller facets so that photoisomerization can take place more easily. The average diameter of each facet on an evaporated gold surface is about 50 nm, whereas the Au particle only has an average 2.5-nm diameter. Thus, the high curvature of the particle should influence the degree of local order in the formation of the SAM on the shell–core composite.<sup>40a</sup>

The quantum yields for photoisomerization of clusters **4** were significantly lower than in those of thiols **2**, which can be most probably ascribed to a competing quenching of the excited chromophore by the metal core in cluster **4**<sup>3–5,15,34c</sup> and to steric hindrance to geometric isomerization when present in the loosely packed cluster.<sup>11</sup>

The <sup>1</sup>H NMR spectrum of the photoproduct from cluster **4** (Figure 2) showed a decreased intensity at 6.9 ppm and an increased intensity at 4.3 ppm, as is consistent with a much less efficient [2 + 2] cyclodimerization of the stilbene moieties in cluster **4**,  $n = 9$ .<sup>5a</sup> Because the solubility of cluster **4** in CH<sub>2</sub>Cl<sub>2</sub> decreased upon lengthening of the linker, only clusters with linker lengths shorter than  $n = 9$  could be observed. The quantum yields of both isomerization ( $\Phi_i$ )<sub>4</sub> and dimerization ( $\Phi_d$ )<sub>4</sub> increased with linker length (Table 1) in the cluster.

**4. Mechanism.** A proposed kinetic sequence for the photoisomerization of thiols **1** and **2** in solution is shown in Scheme 3 in which T, T\*, and C represent a ground-

**Scheme 4. Photoreactions of a Cluster 3 and 4 in Degassed CH<sub>2</sub>Cl<sub>2</sub> Solution upon Photolysis at 350 nm**


state trans isomer, excited-state trans isomer, and cis isomer, respectively, and  $k_i$ ,  $k_t$ , and  $k_f$  are rate constants for isomerization of the excited state of the trans isomer, nonradiative relaxation of the excited state of the trans isomer, and fluorescence emission, respectively. Although slow photodimerization also occurred for clusters **4**, it can be neglected in the initial kinetic analysis because the quantum yield of dimerization was <4% of the quantum yield of isomerization. Steric hindrance to photodimerization thus reduces its quantum yield so significantly that this process can be neglected from a kinetic analysis focusing on fluorescence, even though excitation hopping within an array of tightly packed chromophores may take place readily.

If so, the quantum yields of isomerization of thiols **1** or **2** in solution ( $\Phi_i$ )<sub>1or2</sub> can be expressed as in eq 1,

$$(\Phi_i)_{1or2} = k_i / (k_i + k_t + k_f) \quad (1)$$

where the subscript 1 or 2 defines the photoresponsive reactant.

Photoreactivity of cluster **3** or **4** is described in Scheme 4, where an additional metal-mediated pathway  $k_m$  is included.<sup>15</sup> The quantum yields of isomerization of clusters **3** or **4** on colloidal Au ( $\Phi_i$ )<sub>3or4</sub> can be expressed as in eq 2,

$$(\Phi_i)_{3or4} = k_i / (k_i + k_m + k_t + k_f) \quad (2)$$

where the subscript 3 or 4 defines the chemical identity of the specific cluster and  $k_m$  is the rate constant for quenching of the excited chromophore mediated by the colloidal metal core. If traces of residual tetraoctylammonium bromide remained on the Au core because of incomplete replacement by thiol, the residual bromide ion could quench (at least in principle) the excited chromophore. However, spectral analysis shows that residual tetraoctylammonium bromide is present at far too low a concentration to account for the appreciable quenching observed. In addition, the observed dependence of quenching efficiency on the appended chain length (vide infra) argues against a significant role for the electrolyte whose presence should have been largely independent of chain length.

Because the quantum yields of isomerization for **1** or **2** depend only weakly on linker length, the contribution from the linker itself could be ignored. Assuming that  $k_i$ ,  $k_t$ , and  $k_f$  in clusters **3** and **4** remain unchanged relative to those of thiols **1** and **2**, a combination of eqs 1 and 2 yields eq 3:

$$(\Phi_i)_{1or2} / (\Phi_i)_{3or4} = 1 + k_m / (k_i + k_t + k_f) \quad (3)$$

Because no fluorescence could be observed for the azobenzenes **1** or **3**,  $k_f$  can be ignored. The linker length can be estimated by calculating van der Waals contact

(40) (a) Leopold, M. C. Ph.D. dissertation, North Carolina State University, Raleigh, NC, 2000. (b) Aguila, A.; Murray, R. W. *Langmuir* **2000**, *16*, 5949.



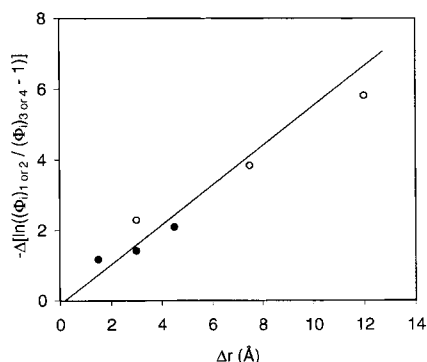


**Figure 9.** Dependence on spacer length of the quantum efficiency for trans to cis isomerization of clusters **3** and **4**: plot of  $-\Delta[\ln((\Phi_i)_{1or2}/(\Phi_i)_{3or4} - 1)]$  against  $\Delta r$ : (○) **3** and (◻) **4**.

distances and by assuming a zigzag conformation for each  $-\text{CH}_2-$  group.

If quenching by the metal cluster takes place by electron transfer or by through-bond electronic interaction,  $k_m$  will generally depend on the donor–acceptor distance as in eq 4,<sup>14,41</sup>

$$k_m = k_0 \exp[-\beta(r - r_0)] \quad (4)$$

where  $r$  is the donor–acceptor distance,  $r_0$  is the van der Waals contact distance separating the centers of the donor and acceptor, and  $\beta$  is a constant that determines the rate of fall-off with distance. Combining eqs 3 and 4, one obtains eq 5

$$\begin{aligned} (k_m)_A/(k_m)_B &= [((\Phi_i)_{1or2})_A/((\Phi_i)_{3or4})_A - 1]/ \\ & \quad [((\Phi_i)_{1or2})_B/((\Phi_i)_{3or4})_B - 1] \\ &= \exp[-\beta(r_A - r_B)] \end{aligned} \quad (5)$$

for chain lengths A and B. Equation 5 can also be expressed as

$$\Delta[\ln((\Phi_i)_{1or2}/(\Phi_i)_{3or4} - 1)] = -\beta\Delta r \quad (6)$$

where  $\Delta r = (r_A - r_B)$  and  $\Delta[\ln((\Phi_i)_{1or2}/(\Phi_i)_{3or4} - 1)] = \ln((\Phi_i)_{1or2}/(\Phi_i)_{3or4} - 1)_A - \ln((\Phi_i)_{1or2}/(\Phi_i)_{3or4} - 1)_B$ .

When  $-\Delta[\ln((\Phi_i)_{1or2}/(\Phi_i)_{3or4} - 1)]$  is plotted against  $\Delta r$ , a roughly linear relationship is obtained (Figure 9), when the cluster **3**,  $n = 4$ , was used as the reference for the azobenzene derivatives **3** or the cluster **4**,  $n = 6$ , was used as the reference for the stilbene derivatives **4**. The slope of the line for clusters **3** almost exactly coincided with that for clusters **4**. From the slope of this line, the  $\beta$  values for both clusters **3** and **4** were estimated as  $0.5 \pm 0.1 \text{ \AA}^{-1}$ .

Because  $\beta$  values for electron transfer through saturated linkages generally range from 0.8 to  $1.2 \text{ \AA}^{-1}$ ,<sup>41,42</sup> the value obtained here may appear to be somewhat low.<sup>43–46</sup> This value is also lower than that observed for

a SAM on a flat Au electrode (0.85),<sup>47–50</sup> but is quite consistent with a  $\beta$  value (0.50) for cyclic thioether spacers used to bind q-CdSe to gold.<sup>51</sup> A possible reason for a low  $\beta$  value is that a bound organic reagent on a metallic core is less rigid conformationally than that on a flat support, where  $\pi$ -stacking is easily achieved.<sup>8</sup> Through-bond electron-transfer quenching of the excited chromophore by the Au core might thus be complicated by contributions reflecting conformations of bound reagents with significant local disorder.<sup>40b</sup> Alternatively, because the chromophores in a partially disordered monolayer have available to them a number of accessible conformers where the distance is greatly reduced from the fully extended molecules, a subpopulation of conformers may provide the observed quenching channel. If so, the apparent  $\beta$  value obtained here would represent a lower limit for the real distance dependence.

The quantum yields for dimerization for clusters **4** also increased upon increasing the linker length (Table 1), likely because quenching of the excited stilbene by the metal core became weaker as the chromophore was positioned further from the metal core. However, even at steady state, only about 15% of the appended stilbene moieties were dimerized, independent of the linker length. Photodimerization is generally believed to take place only when the molecules are properly aligned and within a “magic distance” of 0.35–0.42 nm.<sup>18,28</sup> Only a fraction of the neighboring stilbene moieties in clusters **4** are packed closely enough to dimerize efficiently. We infer that **4** is characterized by loose packing of the thiol on the central Au core<sup>8,11</sup> or that  $\pi$ -stacking is inhibited by the small size of the local facets of the Au colloidal particle.

## Conclusions

Gold clusters capped by alkylthiols with 4–12 carbons and terminal-functionalized with a *trans*-azobenzene or a *trans*-stilbene group were photochemically active upon direct photolysis at 350 nm. Photoisomerizations from the trans to cis isomers were less efficient in the capped clusters **3** and **4** than in the precursor thiols **1** and **2**. The quantum yields for isomerization and dimerization in the clusters **3** and **4** depend on linker chain length, likely because of length-dependent quenching of the excited state by the metallic core. The  $\beta$  value for clusters **3** and **4** estimated as  $0.5 \pm 0.1 \text{ \AA}^{-1}$  is lower than that observed for many through-bond coupling quenchers and may reflect significant disorder in the capped cluster. The stilbene moieties present on clusters **4** could be photodimerized only incompletely (about 15%), prob-

(41) (a) Mikkelsen, K. V.; Ratner, M. A. *Chem. Rev.* **1987**, *87*, 113. (b) Wasielewski, M. R. *Chem. Rev.* **1992**, *92*, 435. (c) Chen, P.; Meyer, T. J. *Chem. Rev.* **1998**, *98*, 1439.

(42) Barbara, P. F.; Meyer, T. J.; Ratner, M. A. *J. Phys. Chem.* **1996**, *100*, 13148.

(43) Ogawa, M. Y.; Wishart, J. F.; Young, Z.; Miller, J. R.; Isied, S. S. *J. Phys. Chem.* **1993**, *97*, 11456.

(44) Barton, J. K.; Kumar, C. V.; Turro, N. J. *J. Am. Chem. Soc.* **1986**, *108*, 6391.

(45) Arkin, M. R.; Stemp, E. D. A.; Jenkins, Y.; Barbara, P. F.; Turro, N. J.; Barton, J. K. *Polym. Mater. Sci. Eng.* **1994**, *71*, 598.

(46) Gust, D.; Moore, T. A.; Liddell, P. A.; Nemeth, G. A.; Makings, L. R.; Moore, A. L.; Barrett, D.; Pessiki, P. J.; Bensaaon, R. V.; Rougee, M.; Chachaty, C.; De Schryver, F. C.; Van der Auweraer, M.; Holzwarth, A. R.; Connolly, J. S. *J. Am. Chem. Soc.* **1987**, *109*, 846.

(47) Slowinski, K.; Chamberlain, R. V.; Miller, C. J.; Majda, M. *J. Am. Chem. Soc.* **1997**, *119*, 11910.

(48) Miller, C.; Cuenet, P.; Graetzel, M. *J. Phys. Chem.* **1991**, *95*, 877.

(49) Finklea, H. O.; Hanshaw, D. D. *J. Am. Chem. Soc.* **1992**, *114*, 3173.

(50) Weber, K.; Hockett, L.; Creager, S. E. *J. Phys. Chem. B* **1997**, *101*, 8286.

(51) Bakkars, E. P. A. M.; Marsman, A. W.; Jennekens, L. W.; VanMaekelbergh, D. *Angew. Chem., Int. Ed.* **2000**, *39*, 2297.



ably because of loose packing of the chromophores on the small surface facets of the metallic colloidal cores.

**Acknowledgment.** This work was supported by the U.S. Department of Energy, Office of Basic Energy Science, Chemistry Division, Fundamental Interactions Branch.

**Supporting Information Available:** Synthesis and spectral data for thiols **1** and **2** and precursors **6** (PDF). This material is available free of charge via the Internet at <http://pubs.acs.org>.

CM000752S